

Variations in soil aggregate stability due to land use changes from agricultural land on the Loess Plateau, China

Guang-yu Zhu^{a,*}, Zhou-ping Shangguan^{b,c}, Lei Deng^{b,c,*}

^a Ministry of Education, Key Laboratory of the Three Gorges Reservoir Region's Ecoenvironment, Chongqing University, Chongqing 400045, PR China

^b State Key Laboratory of Soil Erosion and Dryland Farming on the Loess Plateau, Northwest A&F University, Yangling, Shaanxi 712100, PR China

^c Institute of Soil and Water Conservation, Chinese Academy of Sciences and Ministry of Water Resources, Yangling, Shaanxi 712100, PR China

ARTICLE INFO

Keywords:

Inorganic nitrogen
Soil erosion
Soil particles
Soil structure
Vegetation types

ABSTRACT

Soil aggregate stability is a feasible and effective factor to understand the complex interactions between physicochemical properties and soil structure. To reveal the distributions of soil aggregate stability and its influential factors following land use change from apple orchards abandonment and development in the Nangou watershed of the Loess Plateau, China, this study selected five ages of apple orchards and their planting years were 1 year, 3 years, 6 years, 8 years and 10 years, one 15-year grassland developed from an apple orchard, one 15-year grassland developed from farmland, one natural grassland and one 15-year locust. Results showed that restored vegetation had better soil aggregate stability, soil organic carbon (SOC), and nitrogen (N) than apple orchards, and the composition of soil particles with the best aggregate stability was clay 6%, silt 8%, and sand 86%. At a 0–10 cm soil depth, soil aggregate stability had a significant positive correlation with SOC and soil total nitrogen (STN), and a negative correlation with NO_3^- and NH_4^+ . In addition, vegetation diversity and coverage only affected the soil aggregate stability of the 0–10 cm soil depth; however, soil pH, bulk density, and soil aggregate-associated inorganic nitrogen were the main influential factors that drove the soil aggregate stability of the 0–30 cm soil depth. Further research discovered that macro-aggregate associated NO_3^- and micro-aggregate associated NH_4^+ may be the key factors affecting the soil aggregate stability. Therefore, it is essential to further explore the effect of soil aggregate-associated inorganic nitrogen on soil aggregate stability.

1. Introduction

Soil structure, widely used as an indicator of soil aggregate stability, depends on the arrangement of pores and aggregate water content, which are controlled by the dynamics of the biological activity and physicochemical properties facilitating the formation of soil aggregate (Six et al., 2000). Soil aggregates and their stability, which is regarded as one of the key influential factors, can affect soil water storage, soil carbon storage, soil porosity, interflow, bioactivity (Gallardo-Carrera et al., 2007), soil erosion, and soil quality (Barthès & Roose, 2002; Algayer et al., 2014a; Elhaja et al., 2014). A good and normal soil structure can create a significant improvement in the structure and biodiversity of soil bacterial and fungal communities, nutrient recycling, water availability and vegetation diversity while reducing soil erosion and the rate of increase in CO_2 (Bronick & Lal, 2005; Caplan et al., 2017). During raindrop impact on the soil, aggregates break down and

produce finer, more transportable particles and micro-aggregates (Yan et al., 2008). “The Loess Plateau” is the most severe soil erosion area in the world, and unlimited human activities have significantly shifted its landscape, hydro geography and geomorphic conditions (Zhao et al., 2013). Therefore, soil aggregate stability is a feasible and effective method to evaluate the soil structure, and to understand the complex interactions between the physicochemical properties and soil structure in this region.

According to the hierarchical theory of aggregate formation, soil aggregation is mediated by soil organic matter, the clay content, roots, soil fauna, carbonates, and physical processes, and these materials may be distributed unevenly in different size fractions of soil aggregates (Six et al., 2004; Bronick & Lal, 2005). Based on this, numerous studies have focused on the interactions of aggregate stability with clay (Huang et al., 2016; Medina et al., 2017), soil organic carbon (SOC) (Meersmans et al., 2011; Burrell et al., 2016), vegetation biodiversity and root traits

* Corresponding authors at: No. 83 Shabei Street, Shapingba, Chongqing 400045, PR China (G. Y. Zhu) and No. 26, Xinong Road, Yangling, Shaanxi 712100, PR China (L. Deng).

E-mail addresses: zhu.guangyu@cqu.edu.cn (G.-y. Zhu), leideng@ms.iswc.ac.cn (L. Deng).

<https://doi.org/10.1016/j.catena.2021.105181>

Received 9 July 2020; Received in revised form 7 January 2021; Accepted 13 January 2021

Available online 30 January 2021

0341-8162/© 2021 Published by Elsevier B.V.

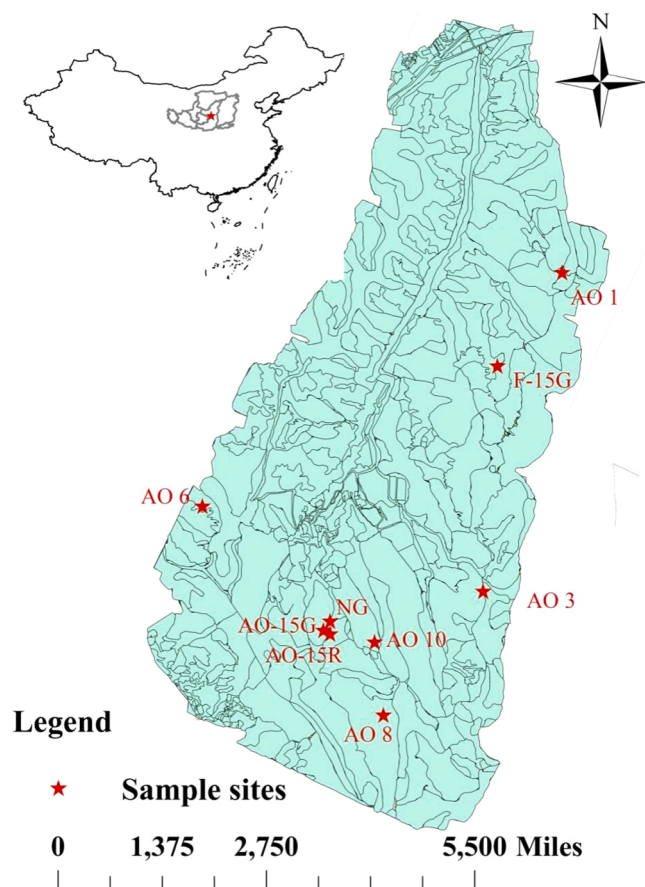


Fig. 1. Location of study site in the Xiaonangou watershed of the Loess Plateau, China. Note: AO 1, 1 year apple orchard; AO 3, 3 years apple orchard; AO 6, 6 years apple orchard; AO 8, 8 years apple orchard; AO-15G, grassland for 15 years abandoned apple orchard; AO-15R, black locust (*Robinia pseudoacacia*) for 15 years abandoned apple orchard; NG, natural grassland.

(Leifheit et al., 2014; Gould et al., 2016; Vergani & Graf, 2016), earthworms (Kohler-Milleret et al., 2013), exchangeable Ca^{2+} and Mg^{2+} (Amézqueta, 1999; Lehtinen et al., 2014), and soil erosion rates (Erktan et al., 2016; Le Bissonnais, 2016; Schweizer et al., 2017) in different land use types. Ecological restoration improves soil biodiversity and

vegetation productivity, and the increase in litter input led to the improvement of soil function (Zhang et al., 2018; Zhong et al., 2018). Generally, the clay content adhered to more organic carbon and humus (Caravaca et al., 2001), and nitrogen and carbon showed a very significant positive correlation, therefore, soil clay and nitrogen also have an important effect on soil aggregates. Numerous indices can be adopted for evaluating soil aggregate stability such as the structural stability index (SI) (Pieri, 2012), fractal dimension (D) (Perfect et al., 1992), mean weight diameter (MWD), geometric mean diameter (GMD), water-stable aggregation (Kemper & Rosenau, 1986), normalized stability index (Six et al., 2004) and whole soil stability index (Nichols & Toro, 2011). Until now, many studies on soil aggregate formation mechanisms, aggregate stability, and aggregate-associated carbon stocks concentrated on land use changes, for instance, other ecosystems to farmland (Eynard et al., 2004; Spohn & Giani, 2011; Sun et al., 2017), farmland to grassland (Wang et al., 2017; Zhao et al., 2017a), and farmland to man-made or natural forest (Qiu et al., 2015; Deng & Shangguan, 2017). However, few researchers have investigated the distributions and influential factors of soil aggregate stability and its relationship with soil properties following land use changes from apple orchard development and abandonment.

In order to consolidate the previous results and further promote ecological construction, the second round of the “Green for Green” Program was launched in China in 2014. However, as the conversion of cropland to forest and grassland is less beneficial than the conversion to another cropland type, some economically viable ecological vegetation conversion has been taken seriously. In China, the Loess Plateau is the main producing area of apple, but limited water resources, a poor soil structure, and nutrient loss have greatly restricted the development of the apple industry in this region. With the purpose of protecting the health of the soil structure in apple orchards and contributing to the top-level design of the conversion of old apple orchards to other ecosystems, the aims of this research were to: (a) estimate the differences in soil aggregate stability indices (SI, D, MWD, GMD); (b) explore the relationships between soil aggregate stability indices and soil properties; and (c) clearly identify the influential factors that affect aggregate stability following land use change from apple orchards abandonment and development. We assumed that the management measures of each apple orchard were basically the same because apple orchards in this area are distributed very close to each other.

Table 1

The general geographical and vegetative features of the investigated sites. Due to the accidental weed interference, AO 3, AO 8 and AO 10 were lack of biological information on the ground.

Sites	Longitude (E)	Latitude (N)	Altitude (m)	R	H	E	Coverage (%)	Height (cm)	Land use details	
Apple orchards	AO 1	109.302	36.604	1214.8	2.67 ± 0.33d	0.56 ± 0.15c	0.56 ± 0.09c	7.66 ± 1.45	13.66 ± 1.20	New terrace, 1 year
	AO 3	109.301	36.589	1272.1	–	–	–	–	–	7 years terrace, 3 years apple orchard
	AO 6	109.282	36.595	1280.6	4.00 ± 0.00d	1.28 ± 0.02b	0.93 ± 0.01a	21.67 ± 1.67c	33.67 ± 1.86ab	9 years terrace,, 6 years
	AO 8	109.294	36.581	1334.6	–	–	–	–	–	12 years terrace, 8 years
locust	AO-15R	109.291	36.586	1254.3	9.00 ± 1.16b	1.41 ± 0.07b	0.65 ± 0.03bc	73.33 ± 1.67a	44.00 ± 2.65ab	30 years apple orchard to 15 years Robinia pseudoacacia
	AO-15G	109.290	36.586	1250.4	9.00 ± 0.00b	1.32 ± 0.05b	0.60 ± 0.02bc	71.67 ± 4.41ab	44.00 ± 4.58ab	30 years apple orchard to 15 years grassland
Grassland	F-15G	109.306	36.610	1183.5	10.33 ± 0.33b	1.22 ± 0.21b	0.52 ± 0.08c	60.00 ± 8.66b	44.33 ± 5.36ab	45 years farmland to 15 years Grassland
	NG	109.291	36.587	1240.8	13.00 ± 1.00a	1.83 ± 0.16a	0.71 ± 0.05b	75.00 ± 2.89a	65.00 ± 2.89a	80 years natural grassland

Note: Values are in the form of the Mean ± SE, and the sample size n = 30. Different lower-case letters mean significant differences in the same soil layers at the different sites ($P < 0.05$). R: Species richness, H: Shannon–Wiener diversity index, E: Evenness index.

Table 2

Soil basic physiochemical properties in the nine sites. Values are in the form of the Mean \pm SE, and the sample size $n = 6$.

Soil depths	Sites	pH	BD	SW
0–10 cm	AO 1	8.59 \pm 0.02a	1.43 \pm 0.00a	0.16 \pm 0.00b
	AO 3	8.53 \pm 0.08a	1.39 \pm 0.00b	0.15 \pm 0.01b
	AO 6	8.53 \pm 0.00a	1.37 \pm 0.00b	0.12 \pm 0.01b
	AO 8	8.403 \pm 0.04a	1.40 \pm 0.01b	0.19 \pm 0.01a
	AO 10	8.50 \pm 0.02a	1.38 \pm 0.02b	0.15 \pm 0.03b
	AO-15R	8.36 \pm 0.00a	1.39 \pm 0.03b	0.19 \pm 0.01a
	AO-15G	8.45 \pm 0.02a	1.38 \pm 0.00b	0.20 \pm 0.02a
	F-15G	8.39 \pm 0.25a	1.38 \pm 0.00b	0.19 \pm 0.01a
	NG	7.69 \pm 0.26b	1.37 \pm 0.01b	0.20 \pm 0.01a
	10–20 cm	AO 1	8.64 \pm 0.03a	1.47 \pm 0.00a
AO 3		8.64 \pm 0.02a	1.42 \pm 0.00b	0.17 \pm 0.01bc
AO 6		8.63 \pm 0.01a	1.36 \pm 0.01d	0.13 \pm 0.00c
AO 8		8.47 \pm 0.05bc	1.41 \pm 0.01bc	0.19 \pm 0.01ab
AO 10		8.58 \pm 0.05ab	1.38 \pm 0.02bcd	0.15 \pm 0.02c
AO-15R		8.43 \pm 0.026c	1.38 \pm 0.02bcd	0.20 \pm 0.01a
AO-15G		8.44 \pm 0.026c	1.38 \pm 0.01 cd	0.20 \pm 0.01a
F-15G		8.41 \pm 0.021c	1.37 \pm 0.01d	0.18 \pm 0.01ab
NG		8.29 \pm 0.08d	1.37 \pm 0.01d	0.19 \pm 0.00ab
20–30 cm		AO 1	8.61 \pm 0.03ab	1.48 \pm 0.00a
	AO 3	8.71 \pm 0.01a	1.43 \pm 0.02b	0.18 \pm 0.02ab
	AO 6	8.63 \pm 0.02ab	1.39 \pm 0.02c	0.15 \pm 0.02ab
	AO 8	8.49 \pm 0.06bc	1.40 \pm 0.01bc	0.19 \pm 0.01a
	AO 10	8.65 \pm 0.03a	1.39 \pm 0.01c	0.14 \pm 0.02b
	AO-15R	8.45 \pm 0.10c	1.40 \pm 0.02bc	0.18 \pm 0.03ab
	AO-15G	8.49 \pm 0.06bc	1.40 \pm 0.02bc	0.17 \pm 0.02ab
	F-15G	8.45 \pm 0.04bc	1.38 \pm 0.01c	0.17 \pm 0.00ab
	NG	8.41 \pm 0.07c	1.37 \pm 0.01c	0.18 \pm 0.01ab

Note: Different lower-case letters mean significant differences in the same soil layers at the different sites ($P < 0.05$).

2. Materials and methods

2.1. Sites

The study site was selected in the Nangou watershed of the Loess Plateau, which has a semi-arid continental climate, covering a total area of 27 km², near Ansai County in Shaanxi Province, China (109°17'3.3432"–109°18'27.7488" E, 36°34'27.66"–36°37'22.62" N) (Fig. 1). The elevations of this hilly-gully region range from 1067.4 to 1334.6 m a.s.l. the mean annual rainfall in this area is 501 mm, the mean annual temperature is 8.8 °C, and the annual sunshine duration is 2397.3 h (1960–2010). The area's soils are classified as *Calcic Cambisols* (IUSS working Group WRB, 2015). In this region, the artificial vegetation types are *Robinia pseudoacacia*, *Hippophae rhamnoides*, *Amygdalus davidiana*, *Malus domestica*, and *Zea mays*, and the natural vegetation types are *Artemisia gmelinii*, *Artemisia scoparia*, *Roegneria kamoji*, *Stipa bungeana*, *Sophora viciifolia* and so on.

Due to the launching of the "Grain for Green" Program and the senescence of apple orchards, the watershed had introduced locust (*Robinia pseudoacacia*) was introduced on abandoned apple orchards; some of the orchards that were not afforested became grasslands through natural succession. After ~ 15 years of vegetation restoration, the undergrowth of locust (*Robinia pseudoacacia*) consisted mainly of *Bothriochloa ischaemum*, *Rubus corchorifolius*, *Plantago depressa*, *Artemisia capillaries*, and so on. The undergrowth of apple orchards was mainly *Cleistogenes caespitosa*, *Setaria viridis*, *Portulaca oleracea*, and so on.

2.2. Samplings and measurements

2.2.1. Experimental design and sampling

Consistent with Zhu et al. (2018), in August 2016, soil samples were obtained when biomass had reached its peak. Nine study sites totaling >1 ha were selected based on the land use change from apple orchard development and abandonment. In the development stage of apple orchards, we chose five ages of apple orchards, 1 year, 3 years, 6 years, 8

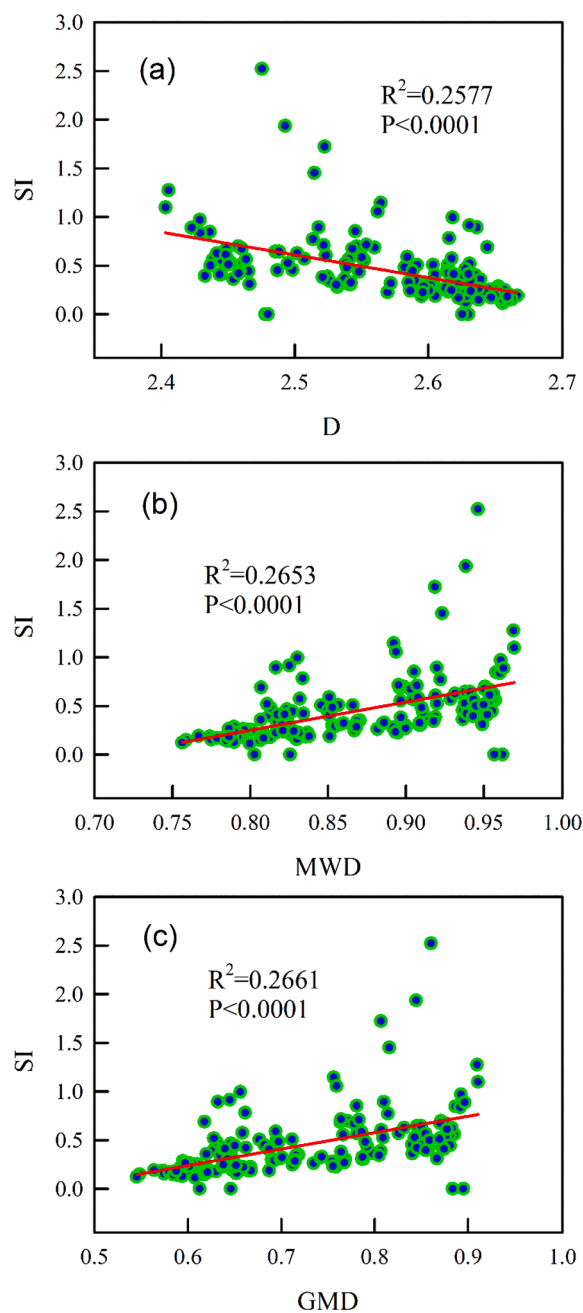


Fig. 2. Relationships between SI and soil aggregate stability indices in 0–30 cm soil depths ($n = 162$). Note: SI indicates accuracy of dry aggregate stability; D, fractal dimension; MWD, mean weight diameter; GMD, geometric mean diameter.

years, and 10 years (AO 1, AO 3, AO 6, AO 8, AO 10); among the abandoned apple orchards, we chose one 15-years grassland developed from an apple orchard (AO-15G), one 15-year grassland developed from farmland (F-15G), one natural grassland and one 15-year locust (AO-15R). Each site has similar geographic and geomorphic conditions. Table 1 shows the detailed information of the nine selected study sites; some plots lack biological information due to accidental interference.

At each site, six 20 m \times 20 m plots were randomly selected to sample soils, and each plot was separated by about 20 m. Five 1 m \times 1 m quadrats, distributed in the center and four corners of each plot, were used to analyze the vegetation community composition, biodiversity, height, and coverage. In total, there were 30 quadrats for each site. This information was used to calculate species richness (R) (Stirling &

Table 3SOC, STN, NN, and AN content of the different soil depths nine sites. Values are in the form of the Mean \pm SE, and the sample size $n = 6$.

Soil depths	Sites	SOC (g kg ⁻¹)	STN (g kg ⁻¹)	NN (mg kg ⁻¹)	AN (mg kg ⁻¹)
0–10 cm	AO 1	2.60 \pm 0.65f	0.28 \pm 0.01f	21.34 \pm 6.27d	7.43 \pm 1.60ab
	AO 3	2.18 \pm 0.21f	0.29 \pm 0.01f	52.07 \pm 3.67 cd	9.62 \pm 2.43ab
	AO 6	3.31 \pm 0.20ef	0.37 \pm 0.02e	45.33 \pm 5.41 cd	7.41 \pm 0.32ab
	AO 8	3.30 \pm 0.19def	0.47 \pm 0.02d	46.04 \pm 2.67 cd	12.71 \pm 3.67a
	AO 10	3.63 \pm 0.18de	0.50 \pm 0.03d	123.13 \pm 42.97b	10.41 \pm 2.16ab
	AO-15R	6.25 \pm 0.18c	0.61 \pm 0.01c	39.67 \pm 2.18 cd	6.21 \pm 0.70b
	AO-15G	5.58 \pm 0.16c	0.59 \pm 0.03c	14.10 \pm 0.54d	7.42 \pm 1.03ab
	F-15G	12.50 \pm 0.68a	1.82 \pm 0.01a	196.67 \pm 22.28a	12.43 \pm 0.42a
	NG	10.96 \pm 0.42b	1.05 \pm 0.03b	73.83 \pm 4.06c	6.84 \pm 1.92b
	10–20 cm	AO 1	2.40 \pm 0.11d	0.27 \pm 0.01f	15.33 \pm 3.13ab
AO 3		2.97 \pm 0.14 cd	0.31 \pm 0.02f	19.31 \pm 0.92ab	6.64 \pm 0.60bc
AO 6		2.35 \pm 0.22d	0.27 \pm 0.01f	17.85 \pm 1.11ab	7.62 \pm 0.60bc
AO 8		3.04 \pm 0.22 cd	0.38 \pm 0.02 cd	22.33 \pm 2.99ab	6.23 \pm 1.41bc
AO 10		3.50 \pm 0.18bc	0.44 \pm 0.02 cd	105.43 \pm 18.05a	12.92 \pm 1.83a
AO-15R		3.48 \pm 0.23bc	0.38 \pm 0.00 cd	20.78 \pm 3.41ab	4.87 \pm 0.80c
AO-15G		4.07 \pm 0.22b	0.45 \pm 0.02c	11.21 \pm 0.52b	8.77 \pm 2.25b
F-15G		7.09 \pm 0.29a	0.97 \pm 0.06a	97.83 \pm 17.88a	10.63 \pm 1.27ab
NG		5.54 \pm 0.29a	0.60 \pm 0.02b	30.20 \pm 1.23ab	4.75 \pm 1.45c
20–30 cm		AO 1	2.66 \pm 0.17c	0.29 \pm 0.01c	13.97 \pm 4.42b
	AO 3	2.41 \pm 0.15c	0.28 \pm 0.02d	12.56 \pm 2.79b	8.23 \pm 2.34bc
	AO 6	2.23 \pm 0.15c	0.26 \pm 0.02d	9.77 \pm 0.51b	9.54 \pm 1.45bc
	AO 8	2.21 \pm 0.16c	0.31 \pm 0.03c	8.58 \pm 1.55b	6.71 \pm 1.70bc
	AO 10	2.89 \pm 0.10c	0.38 \pm 0.01bc	68.67 \pm 20.92a	16.52 \pm 3.84a
	AO-15R	3.09 \pm 0.18c	0.31 \pm 0.01c	10.87 \pm 0.66b	5.04 \pm 1.07c
	AO-15G	3.01 \pm 0.18c	0.34 \pm 0.01c	7.05 \pm 0.33b	10.30 \pm 2.83b
	F-15G	5.42 \pm 0.60a	0.71 \pm 0.07a	56.16 \pm 9.62a	12.32 \pm 2.89ab
	NG	4.10 \pm 0.38b	0.46 \pm 0.05b	21.68 \pm 4.27b	3.72 \pm 1.35c

Note: Different lower-case letters mean significant differences in the same soil layers at the different sites ($P < 0.05$).

Wilsey, 2001), the Shannon–Wiener diversity index (H), and evenness index (E) (Zhu et al., 2016).

There was a total of 6 plots per site to collect 0–30 cm soil samples, and each plot had three replicates. Soil bulk density was obtained using a 5 cm diameter and a 5 cm high stainless steel cutting ring. The soils were dried at 105 °C, and bulk density was calculated when the soil reached a constant weight. Undisturbed soil samples were sealed in lunch boxes and then air dried at laboratory temperature. The air-dried undisturbed soil samples were used to calculate the soil aggregate stability indices, and other physicochemical properties were determined using the remaining soil.

2.2.2. Soil physicochemical properties

Soil pH was measured using a PHS-3C pH acidometer after mixing a 1:5 soil–water ration suspension for 30 min. The SOC content was assayed by the $K_2Cr_2O_7$ – H_2SO_4 oxidation method (Nelson & Sommers, 1996). The TN content was assayed using the Kjeldahl method (Bremner, 1996). Soil NO_3^- (AN) and NH_4^+ (NN) were measured using the method of Bremner & Keeney (1966) to collect the filtrate, and then the filtrate was analyzed for NH_4^+ -N (Crooke & Simpson, 1971) and NO_3^- -N (Best, 1976) with a Continuous Flowing Analyzer (SAN++, SKALAR, Holland). Clay, silt and sand content were determined using a laser particle analyzer (Mastersizer 2000 particle size analyzer, Malvern Instruments, Ltd., UK). Soil BD was calculated by dividing the oven-dried weight by the known volume. The soil water content was measured by oven-drying samples at 105 °C. Table 2 shows the soil pH, soil BD and soil water content of the nine sites.

The > 2.0 mm, 0.25–2 mm and < 0.25 mm soil aggregates were obtained by dry sieving, and SI was used to examine the accuracy of dry sieve method. Macro-aggregates (> 2 mm), middle aggregates (0.25–2 mm) and micro-aggregates (< 0.25 mm) were classified to chemically analyze the soil properties. D, GMD and MWD were calculated based on the results of the soil aggregate size fractions. In this study, because of the very significant linear relationship between SI and soil aggregate stability, dry sieving was an accurate method to estimate D, MWD and GMD (Fig. 2).

Equations as follows:

$$MWD = \sum_{i=1}^n W_i X_i$$

$$GMD = \exp \left[\left(\frac{\sum W_i \log X_i}{\sum W_i} \right) \right]$$

W_i , the proportion of each aggregate class in relation to the bulk soil.
 X_i , the mean diameter of the aggregate class (mm).

$$M(r < R_i) / M_T = (R_i / R_{max})^{3-D_m}$$

M , the cumulative mass of aggregates of i^{th} size r less than R_i .
 M_T , the total mass.
 R_i , the mean aggregate diameter (mm) of the i^{th} size class.
 R_{max} , the mean diameter of the largest aggregate.

$$SI = \frac{1.274 \times SOC}{\text{silt} + \text{clay}} \times 100$$

SI, soil quality indices; SOC, soil organic carbon; Silt, silt content; Clay, clay content.

2.3. Statistical analysis

One-way ANOVA was used to test the differences in vegetation biodiversity and soil physicochemical properties of the nine sites. Two-way ANOVA was used to test the differences among different stages, soil depths, and their interactions. Stepwise multiple regressions were used to create a model of the changes of the influential factors that affected soil aggregate stability following land use change from apple orchards abandonment. Curve fitting was performed, and all images were plotted using the SigmaPlot software program, ver. 12.5. Significant differences were evaluated at the 0.05 level.

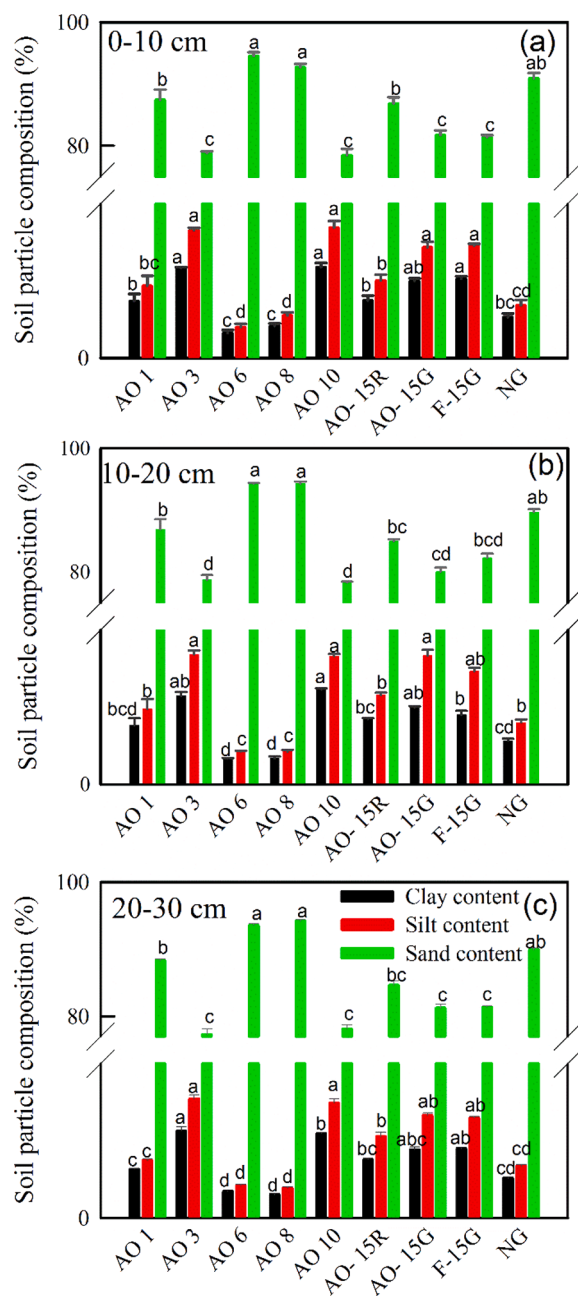


Fig. 3. Effect of nine sites on soil particle composition in 0–30 cm soil depths ($n = 6$). Note: The values are Mean \pm SE. Different lower-case letters mean significant differences in the same soil layers at the different sites ($P < 0.05$).

3. Results

3.1. Soil properties

Generally, following land use change from apple orchards abandonment, STC, STN, NN and AN in restored vegetation were significantly greater than in apple orchards. The increase in the number of apple orchard planting years leads to an increase in STC, STN, NN, and AN, and NG and F-15G were significantly higher than AO-15R and AO-15G (Table 3). The nine sites had the same distribution of STC, STN, AN, and NN at the 10–30 cm soil depths (Table 3).

The clay content (<0.002 mm), silt content (0.002–0.02 mm), and sand content (0.02–2 mm) of the 0–30 cm soil depths varied significantly among the nine sites (Fig. 3). Generally, restored vegetation had a lower sand content than apple orchards, and AO 6 and AO 8 had the

highest sand content at the 0–30 cm soil depth (Fig. 3). The increase in the number of apple orchard planting years led to an increase in the sand content, but the difference in soil particles between restored vegetation was not significant (Fig. 3).

3.2. Soil aggregate composition and soil aggregate stability indices

In general, the most aggregates > 1 mm for the three soil depths were found in AO 1, whereas the fewest were found in AO-15R, AO 10 and F-15G at soil depths of 0–10 cm and 10–30 cm, respectively (Fig. 3 A, B and C). Compared with C-15G, all land use types had significantly more 0.25–1 mm soil aggregates in the soil depths from 0 to 20 cm (Fig. 3, A and B); AO 3 and AO 10 had the most, and AO 1, which had the second lowest recovery of vegetation recovery, had the fewest (Fig. 3, C). In soil depths from 0 to 20 cm, the < 0.25 mm soil aggregates in AO 6 were significantly greater than those in AO 1, AO-15R and C-15G (Fig. 3, A and B). At 20–30 cm soil depths, these aggregates were the highest in AO 10, followed by C-15G and NG, and the fewest were in AO 1 and AO-15R (Fig. 3, C).

In addition, for D at all soil depths, the lowest values were for AO 1 and NG, with the opposite trend for MWD and GMD; AO-15R had the second lowest value and the other treatments were not different (Fig. 3, D). MWD and GMD decreased significantly during the growth of apple orchards at all soil depths (Fig. 3, E and F). However, MWD and GMD in AO-15G, AP-15R and C-15G were not different (Fig. 3, D, E and F).

3.3. Relationships between soil aggregate stability and soil properties

In general, soil aggregate stability had a positive relationship with SOC and TN at the 0–10 cm soil depth (Fig. 5). D showed a negative correlation with SOC and TN (Fig. 5, a and d). MWD and GMD showed a positive relationship with SOC and TN (Fig. 5, b and c). However, the relationship between soil aggregate stability indices and AN and NN had the opposite results (Fig. 6). D showed a positive correlation with AN and NN (Fig. 6, a and d), while MWD and GMD had a negative relationship with AN and NN. Soil particle size fractions had a quadratic parabolic relationship with the soil aggregate stability indices (Fig. 7). D showed no significant correlation with the soil particle size fractions, while MWD and GMD had a downward opening parabolic correlation with the soil particle size fractions. The best soil aggregate stability resulted from 87.5% sand content, 7% silt content and 5.5% clay content.

4. Discussion

4.1. Effects of land use type, soil depths and their interaction on soil properties

In this study, the results showed that the clay content, silt content, sand content and AN were not influenced by soil depth and the interaction of land use change and soil depth, but the rest of the soil properties were significantly influenced by land use change, soil depths and their interactions (Table 4). The previous study of Zhu et al. (2016) demonstrated SOC, STN, AN and NN were consistent with our results, but their results for soil particles were inconsistent. This is mainly because the improvement of soil physical properties will take a long time, and severe soil erosion will interfere with the ecological restoration process (Wang et al., 2018). In addition, Zhu et al. (2017) found that the clay content was not significantly affected by land use change, perhaps because the low plant diversity influenced the bacterial community structure (Lange et al., 2015; Zhang et al., 2015), thereby resulting in clay-organic matter complexes that were not protected from microbial decomposition (Rabbi et al., 2015). Moreover, AN transported with percolating water to the depth cannot be moved back to the soil surface (Aulakh, 1996), and the results showed an even AN distribution in the surface soil (Table 3). Soil aggregate stability indices were

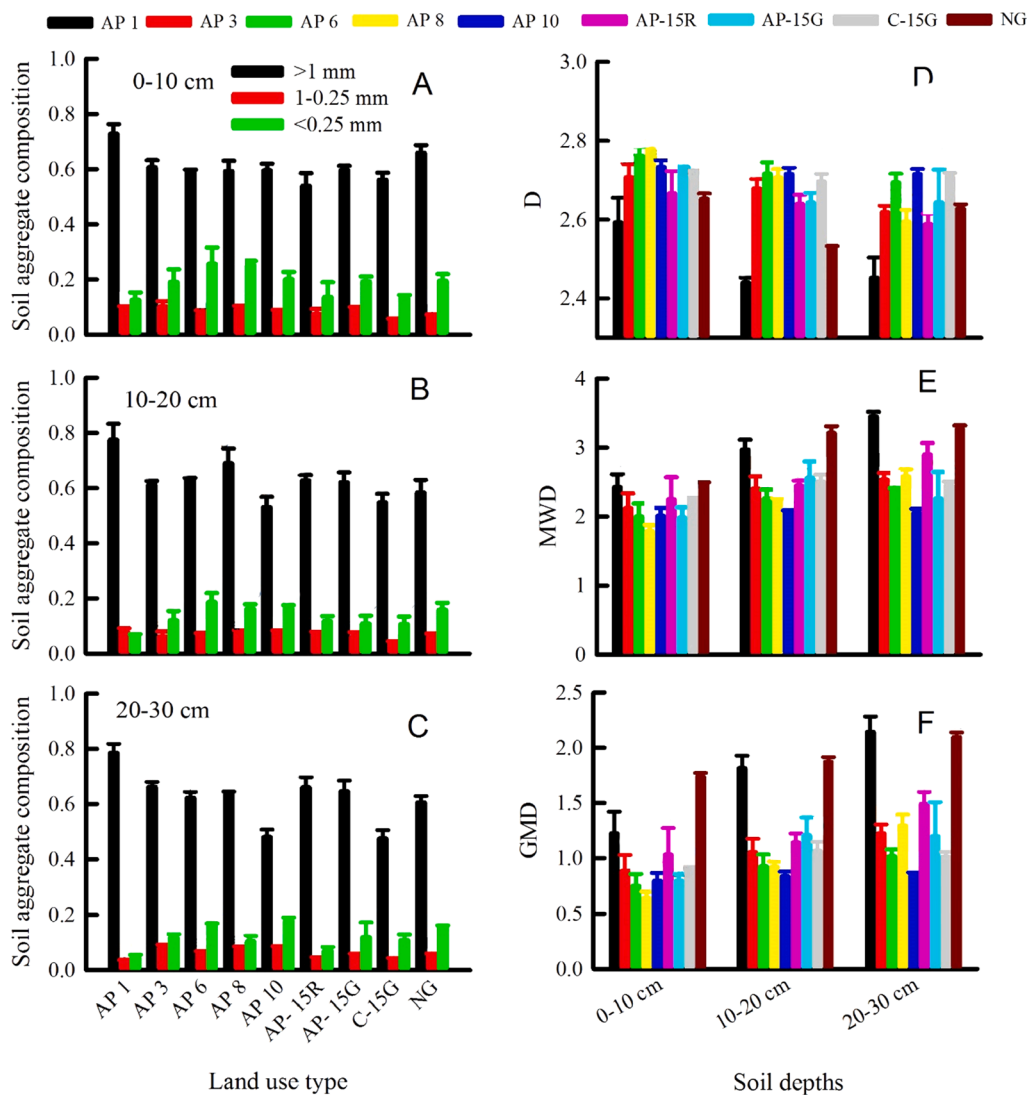


Fig. 4. Effect of nine sites on soil aggregate composition and D, MWD and GMD in 0–30 cm soil depths (n = 6). Note: The values are Mean ± SE. Different lower-case letters mean significant differences in the same soil layers at the different sites (P < 0.05). No significant difference with others is indicated by “n”. D, fractal dimension; MWD, mean weight diameter; GMD, geometric mean diameter.

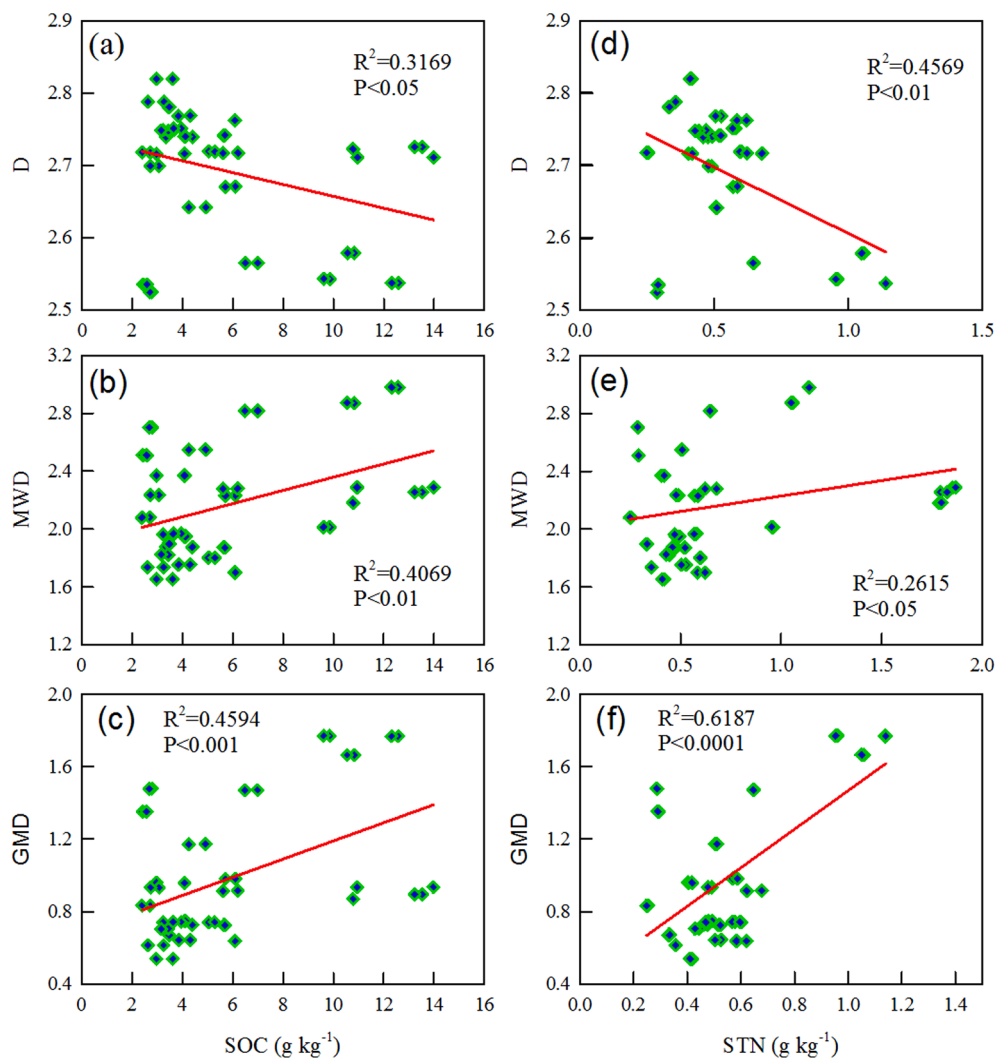


Fig. 5. Relationships between soil aggregate stability indices and SOC and STN in 0–10 cm soil depths ($n = 54$). Note: D, fractal dimension; MWD, mean weight diameter; GMD, geometric mean diameter.

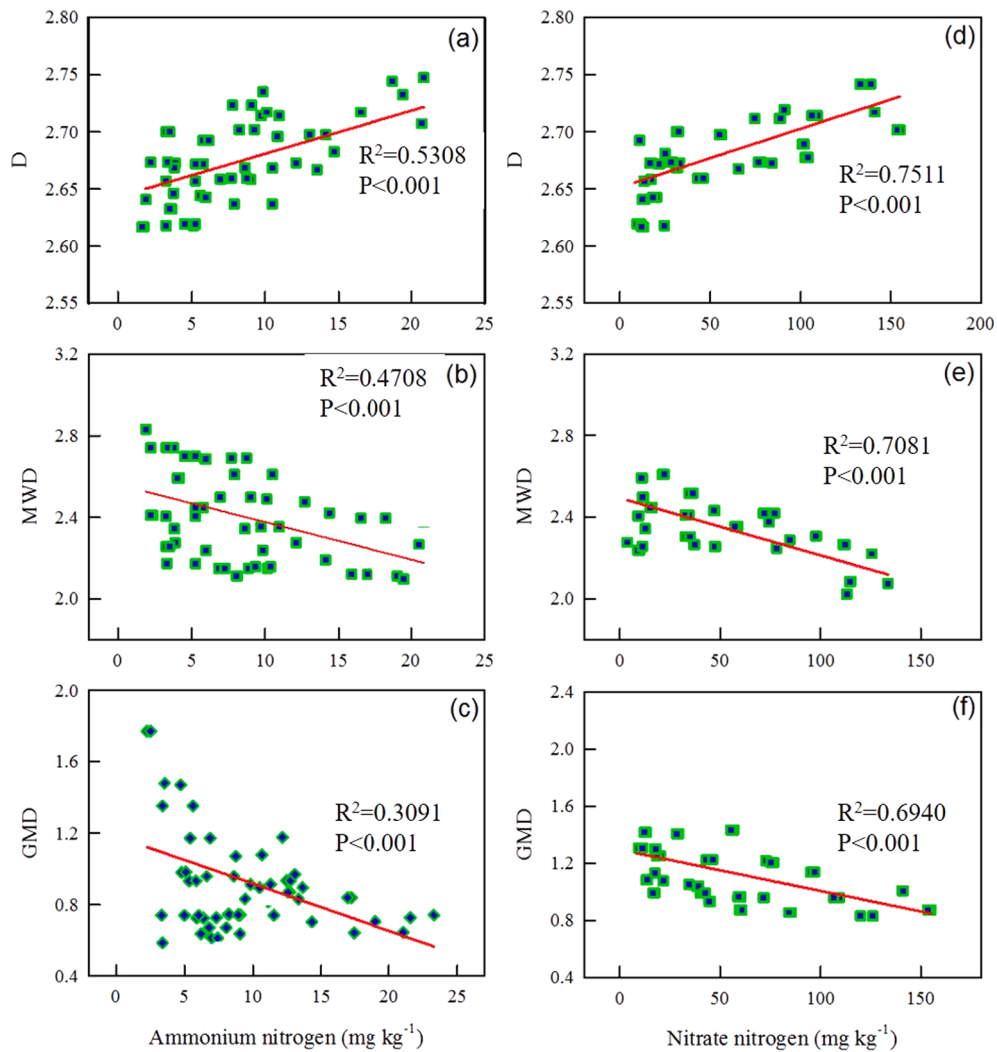


Fig. 6. Relationships between soil aggregate stability indices and AN and NN in 0–10 cm soil depths (n = 54). Note: AN, ammonium nitrogen; NN, nitrate nitrogen; D, fractal dimension; MWD, mean weight diameter; GMD, geometric mean diameter.

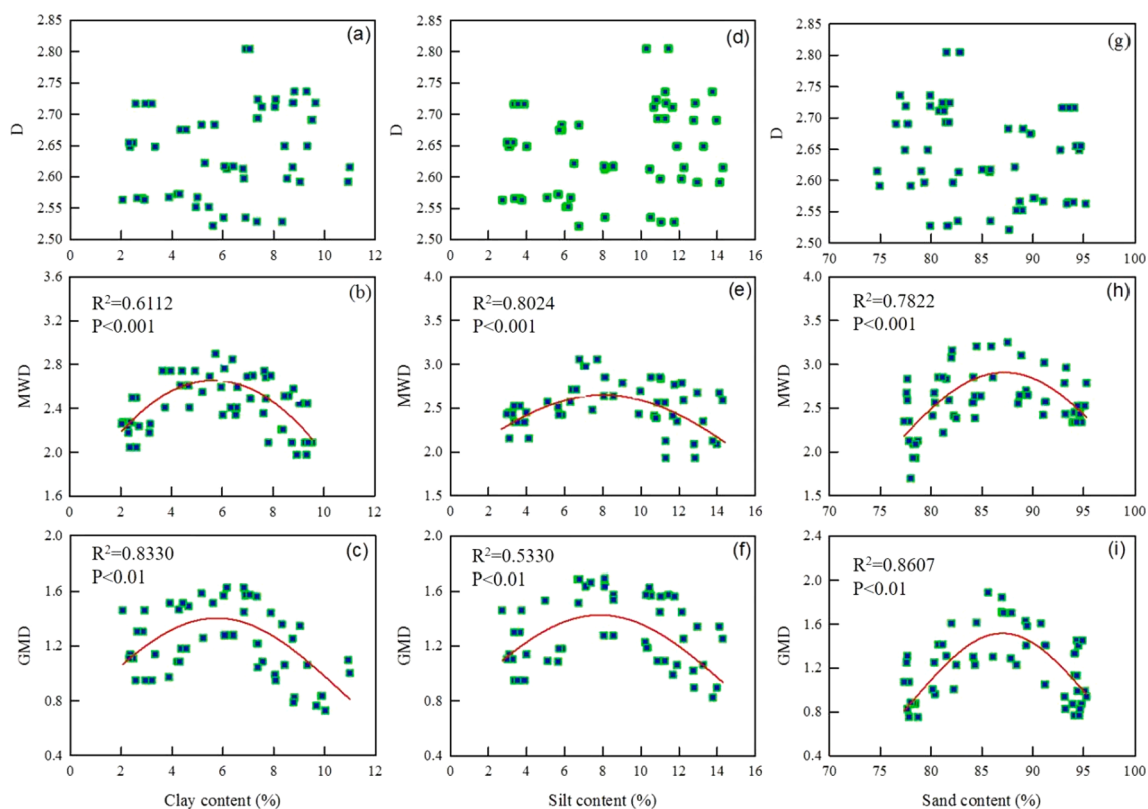


Fig. 7. Relationships between soil particles and soil aggregate stability indices in 0–10 cm soil depths ($n = 54$). Note: D, fractal dimension; MWD, mean weight diameter; GMD, geometric mean diameter.

Table 4

Two-way ANOVA results for the effects of land use type, soil depth and their interaction on soil general properties.

Factor	Variable	df	F	Sig.
Land use type	SOC	7	179.672	0.000**
	STN	7	356.750	0.000**
	AN	7	7.873	0.000**
	NN	7	33.486	0.000**
	Clay	7	164.962	0.000**
	Silt	7	148.875	0.000**
	Sand	7	163.499	0.000**
Soil depth	SOC	2	209.564	0.000**
	STN	2	321.968	0.000**
	AN	2	2.344	0.100
	NN	2	34.984	0.000**
	Clay	2	1.332	0.267
	Silt	2	0.383	0.683
	Sand	2	0.361	0.697
Land use type × Soil depths	SOC	14	27.941	0.000**
	STN	14	49.104	0.000**
	AN	14	1.228	0.263
	NN	14	3.123	0.000**
	Clay	14	0.910	0.550
	Silt	14	0.797	0.671
	Sand	14	0.758	0.712
Soil depths	D	2	21.836	0.000**
	MWD	2	32.957	0.000**
	GMD	2	25.329	0.000**
Land use type	D	7	41.956	0.000**
	MWD	7	20.310	0.000**
	GMD	7	46.775	0.000**
Soil depths × Land use type	D	14	3.767	0.000**
	MWD	14	3.225	0.000**
	GMD	14	9.187	0.000**

Note: Significant differences are indicated by symbols as follows: at * $P < 0.05$ and at ** $P < 0.01$. AN, ammonium nitrogen; NN, nitrate nitrogen; D, fractal dimension; MWD, mean weight diameter; GMD, geometric mean diameter.

significantly affected by land use change, soil depth and their interactions (Table 4). Demenois et al. (2017) also found that soil aggregate stability was influenced by land use change, and plant composition, root traits, and fungal characteristics might explain this result (Faucon et al., 2017). In this study, R and coverage were also important factors that influenced the soil aggregate stability (Table 5). Therefore, a good vegetation environment can stabilize the soil structure. Due to the lack of artificial disturbance after recovery, coupled with the effects of severe soil erosion in an area and root density, the soil aggregate stability of different soil depths can also change (Demenois et al., 2018).

4.2. Distributions of soil properties and aggregate stability

Along with the restoration age since cultivation increased, the soil aggregate stability demonstrated a steeper decrease, and then showed a slowly rising even more than before in all soil depths (Fig. 8). In general, tillage disturbs the soil structure and soil fertility (Nicolas, 2017), and no-tillage cropland or revegetation results in better soil aggregate stability (Nath and Rattan, 2017). For soil tillage in farming, these agricultural activities can increase soil compaction, limiting root frequency, which causes the delamination of soil organic matter and nutrients in the topsoil (Peigné et al., 2018). However, due to the erodible environment, soil nutrients did not stratify in this study (Table 2 and 3). Restored vegetation improved the plant composition and microstructure of soil aggregates (Zhao et al., 2017a). Litter residue of restored vegetation can increase soil organic matter input and improve soil aggregate stability (Fig. 4), especially in the arid and seasonally-dry ecosystems. In total, restored sites had better plant diversity (Table 1) and soil properties (i. e., SOC, N, AN, NN, plant diversity, and coverage) than apple orchards (Table 2 and 3), and these results can provide a basis for controlling soil properties and soil structure by fertilizing and mulching (Mulumba and Lal, 2008).

Table 5
Multiple-regression relations between soil aggregate stability indices and soil properties.

Soil depths (cm)	dependent variable	Formula	R ²
0–10	D	$y = 2.663 + 0.086\text{pH} - 1.821\text{BD} + 0.002\text{MACA}(\text{NN}) - 0.009\text{R}$	0.636**
	MWD	$y = 6.564 - 0.855\text{pH} + 7.446\text{BD} + 0.526\text{E} - 0.050\text{MACA}(\text{NN})$	0.687**
	GMD	$y = -1.324 + 5.964\text{BD} - 0.015\text{AN} - 0.004\text{MACA}(\text{NN}) + 0.153\text{SOC} - 0.123\text{pH}$	0.774**
10–20	D	$y = 3.284 - 1.754\text{BD} + 0.002\text{MICA}(\text{NN}) - 0.016\text{R} + 0.001\text{Coverage} + \text{MICA}(\text{N})$	0.821**
	MWD	$y = -6.852 + 5.346\text{BD} + 0.056\text{R} - 0.038\text{MICA}(\text{NN}) + 0.831\text{pH} + 0.024\text{MIA}(\text{NN})$	0.684*
	GMD	$y = -1.101 - 0.008\text{MICA}(\text{NN}) + 5.997\text{BD} + 0.082\text{R} - 0.005\text{Coverage} - 1.224\text{MICA}(\text{N})$	0.838*
20–30	D	$y = 3.251 - 1.101\text{BD} - 6.433\text{E} - 5 - 0.842\text{SW}$	0.494**
	MWD	$y = -0.854 + 6.898\text{BD} + 0.114\text{Silt} + 0.040\text{MICA}(\text{AN})$	0.593**
	GMD	$y = -2.209 + 7.311\text{BD} - 0.093\text{Sand} + 0.034\text{MICA}(\text{AN})$	0.637**
0–30	D	$y = 2.511 - 1.821\text{BD} - 0.011\text{R} + 0.002\text{MACA}(\text{NN}) + 0.097\text{pH} + 0.003\text{AN} + 0.001\text{Coverage}$	0.616**
	MWD	$y = -0.658 + 7.717\text{BD} + 0.063\text{R} - 0.013\text{MACA}(\text{NN}) - 0.004\text{Coverage} + 0.006\text{MICA}(\text{NN})$	0.557**
	GMD	$y = 2.478 + 7.430\text{BD} + 0.053\text{R} - 0.006\text{MACA}(\text{NN}) - 0.491\text{pH} - 0.004\text{Coverage} - 0.008\text{AN}$	0.624**

Note: Best fits obtained by stepwise multiple-regression. Significant at * $P < 0.05$ and at ** $P < 0.01$ and the coefficients of the included variables are significant at $p < 0.05$. MACA (NN), macroaggregate associated nitrate nitrogen; MICA(NN), middle aggregate associated nitrate nitrogen; MIA(NN), microaggregate associated nitrate nitrogen; R, richness; E, evenness; AN, ammonium nitrogen; NN, nitrate nitrogen.

4.3. Correlation of soil properties with soil aggregate stability

Due to the relatively short period of land use change, biophysical and chemical activities were mainly concentrated on the surface soil; thus, we only showed the relationships between soil properties and soil aggregate stability indices for the 0–10 cm soil depth (Figs. 5, 6 and 7). Plenty of studies found significant positive relationships between the SOC and soil aggregate stability (Blanco-Canqui and Lal, 2007; D'Acqui et al., 2017; Zhao et al., 2017b), consistent with ours (Fig. 5), because SOC is an important material component of soil aggregate formation (Eynard et al., 2005). SOC and STN had a similar tendency as soil aggregate stability due to the coupling effects of SOC and STN (Tong et al., 2009). However, AN and NN had a negative correlation with soil aggregate stability (Fig. 6), and Table 5 shows that macro-aggregate-associated nitrate nitrogen MACA (NN) was the main factor that affected soil aggregate stability. A soluble N in soil is closely related to a decrease in bacterial abundance, it can suppress microbes that carry nitrogen-fixing genes (Pereg et al., 2018), and biological aggregating agents associated with the microbial population have an effect on soil aggregate stability (Tang et al., 2011).

Several studies indicated that there were no relationships between soil particles and soil aggregate stability indices (Algayer et al., 2014b; Lu et al., 2014); some studies found a linear correlation (Regelink et al., 2015). However, this study showed a downward opening parabolic relationship (Fig. 7), probably because swelling clay began to improve when clay reaches the peak which can disrupt aggregates (Bronick & Lal, 2005). In addition, due to the concentrated rainfall and erosion of the Loess Plateau, litter and soil nutrients are also prone to loss, which also leads to this result.

Stepwise regression revealed that BD was the main factor affecting the soil aggregate stability indices at all soil depths (Table 5). Soil BD may include the enrichment in labile organic fractions that are hygroscopic and can bind soil particles into temporary aggregates (Mora & Lázaro, 2014), meanwhile, low soil BD can increase root proliferation, water retention capacity and soil porosity (Tayyab et al., 2018). In

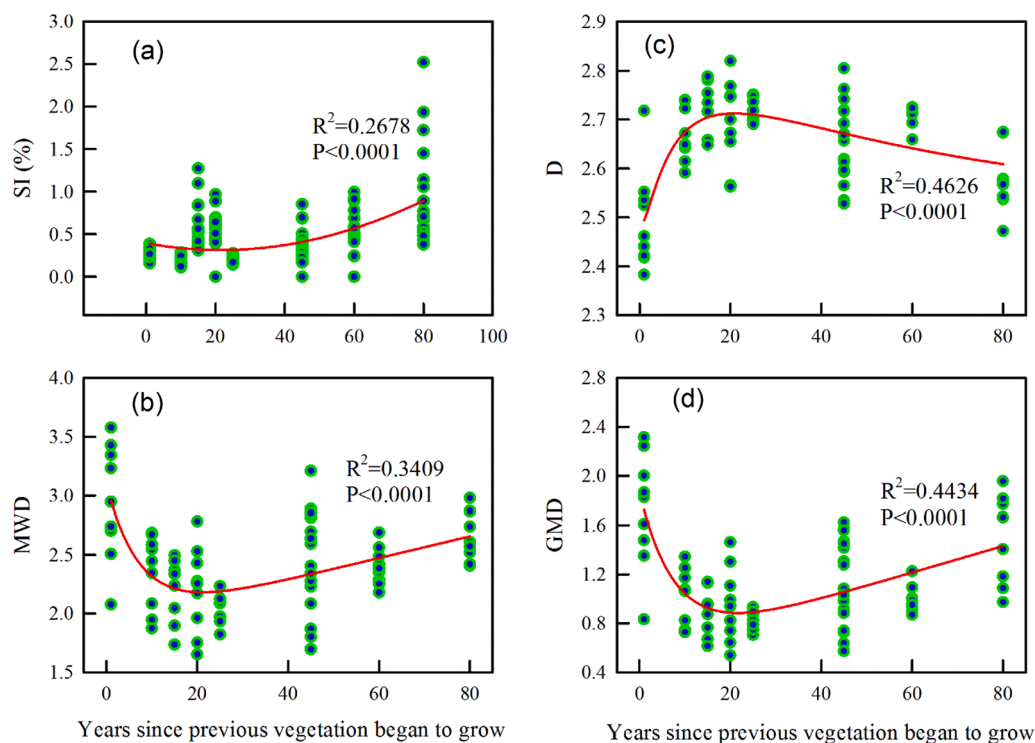


Fig. 8. Relationships between soil aggregate stability indices and restoration age since previous vegetation began to grow in 0–30 cm soil depths ($n = 162$). Note: SI indicates accuracy of dry aggregate stability; D, fractal dimension; MWD, mean weight diameter; GMD, geometric mean diameter.

addition, inconsistent with the research of Bronick and Lal (2005), soil aggregate stability was only affected by soil pH in 0–10 cm in this study (Table 5). Mainly because soil pH can stabilize soil through lots of litter residue in the surface, thereby promoting microbial activity and improving soil aggregate stability (Egan et al., 2018).

In total, it is feasible to control the stability of orchard soil aggregates through management measures such as applying nitrogen fertilizer, planting green manure, and little or no tillage, because soil carbon to nitrogen ratio, soil bulk density, soil pH and so on are changed. Additionally, Combined with Fig. 8, we believe that from the perspective of soil erosion, apple tree planting here is feasible.

5. Conclusions

Land use change and soil physical and chemical properties had an impact on soil aggregate stability, and the soil aggregate stability of restored vegetation was higher than that of artificial vegetation. The composition of the soil particles with the best aggregation stability in the loess hilly area was clay 6%, silt 8% and sand 86%. However, the sand content of the Loess Plateau exceeds 90%, so it is also important to control soil erosion through vegetation restoration. The results showed that soil structure will recovery in a short time after the return of apple orchards to forest and grassland, so apple plantation is worth promoting in the loess hilly region. In addition, SOC, STN, NO_3^- , and NH_4^+ had respective positive, positive, negative, and negative correlations with soil aggregate stability in the surface soil. NO_3^- and NH_4^+ may be the key factors affecting the soil aggregate stability in this semi-arid area, especially the macro-aggregate associated NO_3^- and micro-aggregate associated NH_4^+ . Thus, it is essential to further explore the effect of soil aggregate-associated inorganic nitrogen on soil aggregate stability to maintain the balance of soil properties and the soil structure.

Declaration of Competing Interest

The authors declare that they have no known competing financial interests or personal relationships that could have appeared to influence the work reported in this paper.

Acknowledgements

This study was funded by the National Natural Science Foundation of China (41877538), Open Fund of State Key Laboratory of Soil Erosion and Dryland Farming on the Loess Plateau, Institute of Water and Soil Conservation, Chinese Academy of Sciences and Ministry of Water Resources (A314021402-2004), National Key Research and Development Program of China (2016YFC0501605), the Funding of Special Support Plan of Young Talents Project of Shaanxi Province in China, the Funding of Promoting Plan to Creative talents of 'Youth Science and Technology Star' in Shaanxi Province of China (2018KJXX-088). We thank LetPub (www.letpub.com) for its linguistic assistance during the preparation of this manuscript.

References

Algayer, B., Le Bissonnais, Y., Darboux, F., 2014a. Short-Term Dynamics of Soil Aggregate Stability in the Field. *Soil Sci. Soc. Am. J.* 78, 1168–1176. <https://doi.org/10.2136/sssaj2014.01.0009>.

Algayer, B., Wang, B., Bourennane, H., Zheng, F., Duval, O., Li, G., Le Bissonnais, Y., Darboux, F., 2014b. Aggregate stability of a crusted soil: differences between crust and sub-crust material, and consequences for interrill erodibility assessment. An example from the Loess Plateau of China. *Eur. J. Soil Sci.* 65, 325–335. <https://doi.org/10.1111/ejss.12134>.

Amézketa, E., 1999. Soil Aggregate Stability: A Review. *J. Sustain. Agric.* 14, 83–151. https://doi.org/10.1300/J064v14n02_08.

Aulakh, M.S., 1996. Nitrogen losses and fertilizer N use efficiency in irrigated porous soils. *Nutr. Cycl. Agroecosyst.* 47, 197–212. <https://doi.org/10.1007/BF01986275>.

Barthés, B., Roose, E., 2002. Aggregate stability as an indicator of soil susceptibility to runoff and erosion; validation at several levels. *Catena* 47, 133–149. [https://doi.org/10.1016/S0341-8162\(01\)00180-1](https://doi.org/10.1016/S0341-8162(01)00180-1).

Best, E.K., 1976. An automated method for determining nitrate nitrogen in soil extracts. *Queensland J. Agric. Anim. Sci.*

Blanco-Canqui, H., Lal, R., 2007. Soil structure and organic carbon relationships following 10 years of wheat straw management in no-till. *Soil Tillage Res.* 95, 240–254. <https://doi.org/10.1016/j.still.2007.01.004>.

Bremner, J., 1996. Nitrogen-total. *Methods of Soil Analysis Part 3—Chemical Methods*, 1085–1121. <http://doi.org/10.1016/B978-0-12-386454-3.00522-4>.

Bremner, J., Keeney, D., 1966. Determination and isotope-ratio analysis of different forms of nitrogen in soils: 3. Exchangeable ammonium, nitrate, and nitrite by extraction-distillation methods. *Soil Sci. Soc. Am. J.* 30, 577–582. <https://doi.org/10.2136/sssaj1967.03615995003100030011x>.

Bronick, C.J., Lal, R., 2005. Soil structure and management: a review. *Geoderma* 124, 3–22. <https://doi.org/10.1016/j.geoderma.2004.03.005>.

Burrell, L.D., Zehetner, F., Rampazzo, N., Wimmer, B., Soja, G., 2016. Long-term effects of biochar on soil physical properties. *Geoderma* 282, 96–102. <https://doi.org/10.1016/j.geoderma.2016.07.019>.

Caplan, J.S., Giménez, D., Subroy, V., Heck, R.J., Prior, S.A., Runion, G.B., Torbert, H.A., 2017. Nitrogen-mediated effects of elevated CO₂ on intra-aggregate soil pore structure. *Glob. Change Biol.* 4, 1585–1597. <https://doi.org/10.1111/gcb.13496>.

Caravaca, F., Lax, A., Albaladejo, J., 2001. Soil aggregate stability and organic matter in clay and fine silt fractions in urban refuse-amended semiarid soils. *Soil Sci. Soc. Am. J.* 65, 1235–1238. <https://doi.org/10.2136/sssaj2001.6541235x>.

Crooke, W., Simpson, W., 1971. Determination of ammonium in Kjeldahl digests of crops by an automated procedure. *J. Sci. Food Agric.* 22, 9–10. <https://doi.org/10.1002/jsfa.2740220104>.

D'Acqui, L.P., Bonetti, A., Pini, R., Certini, G., 2017. Physical protection of organic matter in minesols assessed by low-temperature ashing (LTA). *Geoderma* 288, 120–129. <https://doi.org/10.1016/j.geoderma.2016.11.009>.

Demenois, J., Rey, F., Ibanez, T., Stokes, A., Carriconde, F., 2018. Linkages between root traits, soil fungi and aggregate stability in tropical plant communities along a successional vegetation gradient. *Plant Soil* 424, 319–334. <https://doi.org/10.1007/s11104-017-3529-x>.

Demenois, J., Carriconde, F., Rey, F., Stokes, A., 2017. Tropical plant communities modify soil aggregate stability along a successional vegetation gradient on a Ferralsol. *Ecol. Eng.* 109, 161–168. <https://doi.org/10.1016/j.ecoleng.2017.07.027>.

Deng, L., Shanguan, Z.P., 2017. Afforestation drives soil carbon and nitrogen changes in China. *Land Degrad. Dev.* 28, 151–165. <https://doi.org/10.1002/ldr.2537>.

Egan, G., Crawley, M.J., Fornara, D.A., 2018. Effects of long-term grassland management on the carbon and nitrogen pools of different soil aggregate fractions. *Sci. Total Environ.* 613, 810–819. <https://doi.org/10.1016/j.scitotenv.2017.09.165>.

Elhaja, M.E., Ibrahim, I.S., Adam, H.E., Csaplovics, E., 2014. Soil aggregate stability and wind erodible fraction in a semi-arid environment of White Nile State, Sudan. *Land Surf. Remote Sens.* II 9260. https://doi.org/10.1117/12.2069182_926017-926017.

Erktan, A., Legout, C., De Danieli, S., Daumergue, N., Cécillon, L., 2016. Comparison of infrared spectroscopy and laser granulometry as alternative methods to estimate soil aggregate stability in Mediterranean badlands. *Geoderma* 271, 225–233. <https://doi.org/10.1016/j.geoderma.2016.02.025>.

Eynard, A., Schumacher, T.E., Lindstrom, M.J., Malo, D.D., 2004. Aggregate sizes and stability in cultivated South Dakota prairie Ustolls and Usterts. *Soil Sci. Soc. Am. J.* 68, 1360–1365. <https://doi.org/10.2136/sssaj2004.1360>.

Eynard, A., Schumacher, T.E., Lindstrom, M.J., Malo, D.D., 2005. Effects of agricultural management systems on soil organic carbon in aggregates of Ustolls and Usterts. *Soil Tillage Res.* 81, 253–263. <https://doi.org/10.1016/j.still.2004.09.012>.

Faucou, M.P., Houben, D., Lambers, H., 2017. Plant functional traits: soil and ecosystem services. *Trends Plant Sci.* 22, 385–394. <https://doi.org/10.1016/j.tplants.2017.01.005>.

Gallardo-Carrera, A., Léonard, J., Duval, Y., Dürr, C., 2007. Effects of seedbed structure and water content at sowing on the development of soil surface crusting under rainfall. *Soil Tillage Res.* 95, 207–217. <https://doi.org/10.1016/j.still.2007.01.001>.

Gould, I.J., Quinton, J.N., Weigelt, A., De Deyn, G.B., Bardgett, R.D., 2016. Plant diversity and root traits benefit physical properties key to soil function in grasslands. *Ecol. Lett.* 19, 1140–1149. <https://doi.org/10.1111/ele.12652>.

Huang, X.R., Li, H., Li, S., Xiong, H.L., Jiang, X.J., 2016. Role of cationic polarization in humus-increased soil aggregate stability. *Eur. J. Soil Sci.* 67, 341–350. <https://doi.org/10.1111/ejss.12342>.

IUSS Working Group WRB, 2015. World reference base for soil resources 2014, update 2015 international soil classification system for naming soils and creating legends for soil maps. *World Soil Resour. Reports* 106, 192.

Kemper, W.D., Rosenau, R.C., 1986. Aggregate Stability and Size Distribution. In: *Methods of Soil Analysis, Part 1. Physical and Mineralogical Methods* (2nd Edition). *Agron. Monogr.*, 9, 425–442. <http://doi.org/10.2136/sssabookser5.1.2ed.c17>.

Kohler-Milleret, R., Le Bayon, R.C., Chenu, C., Gobat, J.M., Boivin, P., 2013. Impact of two root systems, earthworms and mycorrhizae on the physical properties of an unstable silt loam Luvisol and plant production. *Plant Soil* 370, 251–265. <https://doi.org/10.1007/s11104-013-1621-4>.

Lange, M., Eisenhauer, N., Sierra, C.A., Bessler, H., Engels, C., Griffiths, R.I., Perla, G., Mellado-Vázquez, A.A., Malik, J., Roy, S., Scheu, S., Steinbeiss, B.C., Thomson, S.E., Gleixner, Trumbore G., 2015. Plant diversity increases soil microbial activity and soil carbon storage. *Nat. Commun.* 6, 6707. <https://doi.org/10.1038/ncomms7707>.

Le Bissonnais, Y., 2016. Aggregate stability and assessment of soil crustability and erodibility: I. Theory and methodology. *Eur. J. Soil Sci.* 67, 11–21. <https://doi.org/10.1111/ejss.4.12311>.

Lehtinen, T., Lair, G.J., Mentler, A., Gisladottir, G., Ragnarsdottir, K.V., Blum, W.E.H., 2014. Soil Aggregate Stability in Different Soil Orders Quantified by Low Dispersive Ultrasonic Energy Levels. *Soil Sci. Soc. Am. J.* 78, 713–723. <https://doi.org/10.2136/sssaj2013.02.0073>.

- Leifheit, E.F., Veresoglou, S.D., Lehmann, A., Morris, E.K., Rillig, M.C., 2014. Multiple factors influence the role of arbuscular mycorrhizal fungi in soil aggregation—a meta-analysis. *Plant Soil* 374, 523–537. <https://doi.org/10.1007/s11104-013-1899-2>.
- Lu, S.G., Malik, Z., Chen, D.P., Wu, C.F., 2014. Porosity and pore size distribution of Ultisols and correlations to soil iron oxides. *Catena* 123, 79–87. <https://doi.org/10.1016/j.catena.2014.07.010>.
- Medina, H., van Lier, Q.D., Garcia, J., Ruiz, M.E., 2017. Regional-scale variability of soil properties in Western Cuba. *Soil Tillage Res.* 166, 84–99. <https://doi.org/10.1016/j.still.2016.10.009>.
- Meersmans, J., van Wesemael, B., Goidts, E., van Molle, M., De Baets, S., De Ridder, F., 2011. Spatial analysis of soil organic carbon evolution in Belgian croplands and grasslands, 1960–2006. *Glob. Change Biol.* 17, 466–479. <https://doi.org/10.1111/j.1365-2486.2010.02183.x>.
- Mora, J.L., Lázaro, R., 2014. Seasonal changes in bulk density under semiarid patchy vegetation: the soil beats. *Geoderma* 235–236, 30–38. <https://doi.org/10.1016/j.geoderma.2014.06.022>.
- Mulumba, L.N., Lal, R., 2008. Mulching effects on selected soil physical properties. *Soil Tillage Res.* 98, 106–111. <https://doi.org/10.1016/j.still.2007.10.011>.
- Nath, A.J., Rattan, L.A.L., 2017. Effects of tillage practices and land use management on soil aggregates and soil organic carbon in the north Appalachian region, USA. *Pedosphere* 27, 172–176. [https://doi.org/10.1016/S1002-0160\(17\)60301-1](https://doi.org/10.1016/S1002-0160(17)60301-1).
- Nelson, D.W., Sommers, L.E., 1996. Total carbon, organic carbon, and organic matter. *Methods of soil analysis part 3—chemical methods*, 961–1010. <http://doi.org/10.2136/sssabookser5.3.c34>.
- Nichols, K.A., Toro, M., 2011. A whole soil stability index (WSSI) for evaluating soil aggregation. *Soil Tillage Res.* 111, 99–104. <https://doi.org/10.1016/j.still.2010.08.014>.
- Nicolas, P.A., 2017. Soil fertility after 10 years of conservation tillage in organic farming. *Soil Tillage Res.* 175, 194–204. <https://doi.org/10.1016/j.still.2017.09.008>.
- Pereg, L., Morugán-Coronado, A., Mcmillan, M., García-Orenes, F., 2018. Restoration of nitrogen cycling community in grapevine soil by a decade of organic fertilization. *Soil Tillage Res.* 179, 11–19. <https://doi.org/10.1016/j.still.2018.01.007>.
- Perfect, E., Rasiah, V., Kay, B., 1992. Fractal dimensions of soil aggregate size distributions calculated by number and mass. *Soil Sci. Soc. Am. J.* 56, 1407–1409. <https://doi.org/10.2136/sssaj1992.03615995005600050012x>.
- Peigné, J., Vian, J.F., Payet, V., Saby, N.P., 2018. Soil fertility after 10 years of conservation tillage in organic farming. *Soil Tillage Res.* 175, 194–204. <https://doi.org/10.1016/j.still.2017.09.008>.
- Pieri, C.J., 2012. *Fertility of soils: a future for farming in the West African savannah*. Springer Science & Business Media.
- Qiu, L.P., Wei, X.R., Gao, J.L., Zhang, X.C., 2015. Dynamics of soil aggregate-associated organic carbon along an afforestation chronosequence. *Plant Soil* 391, 237–251. <https://doi.org/10.1007/s11104-015-2415-7>.
- Rabbi, S.M.F., Tighe, M., Delgado-Baquerizo, M., Cowie, A., Robertson, F., Dalal, R., Mcleod, M., 2015. Climate and soil properties limit the positive effects of land use reversion on carbon storage in Eastern Australia. *Sci. Rep.* 5, 17866. <https://doi.org/10.1038/srep17866>.
- Regelink, I.C., Stoof, C.R., Rouseva, S., Weng, L., Lair, G.J., Kram, P., Nikolaidis, N.P., Kercheva, M., Banwart, S., Comans, R.N.J., 2015. Linkages between aggregate formation, porosity and soil chemical properties. *Geoderma* 247–248, 24–37. <https://doi.org/10.1016/j.geoderma.2015.01.022>.
- Schweizer, S.A., Fischer, H., Haring, V., Stahr, K., 2017. Soil structure breakdown following land use change from forest to maize in Northwest Vietnam. *Soil Tillage Res.* 166, 10–17. <https://doi.org/10.1016/j.still.2016.09.010>.
- Six, J., Elliott, E., Paustian, K., 2000. Soil structure and soil organic matter II. A normalized stability index and the effect of mineralogy. *Soil Sci. Soc. Am. J.* 64, 1042–1049. <https://doi.org/10.2136/sssaj2000.6431042x>.
- Six, J., Bossuyt, H., Degryze, S., Denef, K., 2004. A history of research on the link between (micro)aggregates, soil biota, and soil organic matter dynamics. *Soil Tillage Res.* 79, 7–31. <https://doi.org/10.1016/j.still.2004.03.008>.
- Spohn, M., Giani, L., 2011. Impacts of land use change on soil aggregation and aggregate stabilizing compounds as dependent on time. *Soil Biol. Biochem.* 43, 1081–1088. <https://doi.org/10.1016/j.soilbio.2011.01.029>.
- Stirling, G., Wilsey, B., 2001. Empirical relationships between species richness, evenness, and proportional diversity. *Am. Nat.* 158, 286–299. <https://doi.org/10.1086/321317>.
- Sun, D.S., Li, K.J., Bi, Q.F., Zhu, J., Zhang, Q.C., Jin, C.W., Lu, L.L., Lin, X.Y., 2017. Effects of organic amendment on soil aggregation and microbial community composition during drying-rewetting alternation. *Sci. Total Environ.* 574, 735–743. <https://doi.org/10.1016/j.scitotenv.2016.09.112>.
- Tang, J.Y.M., Zhang, J., Zhang, R., 2011. Influence of biological aggregating agents associated with microbial population on soil aggregate stability. *Appl. Soil Ecol.* 47, 153–159. <https://doi.org/10.1016/j.apsoil.2011.01.001>.
- Tayyab, M., Islam, W., Khalil, F., Ziqin, P., Caifang, Z., Arafat, Y., Tarin, M.W.K., 2018. Biochar: An efficient way to manage low water availability in plants. *Appl. Ecol. Environ. Res.* 16, 2565–2583. https://doi.org/10.15666/aer/1603_25652583.
- Tong, C., Xiao, H., Tang, G., Wang, H., Huang, T., Xia, H., Keith, S.J., Li, Y., Liu, S., Wu, J., 2009. Long-term fertilizer effects on organic carbon and total nitrogen and coupling relationships of C and N in paddy soils in subtropical China. *Soil Tillage Res.* 106, 8–14. <https://doi.org/10.1016/j.still.2009.09.003>.
- Vergani, C., Graf, F., 2016. Soil permeability, aggregate stability and root growth: a pot experiment from a soil bioengineering perspective. *Ecology* 9, 830–842. <https://doi.org/10.1002/eco.1686>.
- Wang, H., Zhang, G.H., Li, N.N., Zhang, B.J., Yang, H.Y., 2018. Soil erodibility influenced by natural restoration time of abandoned farmland on the Loess Plateau of China. *Geoderma* 325, 18–27. <https://doi.org/10.1016/j.geoderma.2018.03.037>.
- Wang, R., Dorodnikov, M., Dijkstra, F.A., Yang, S., Xu, Z., Li, H., Jiang, Y., 2017. Sensitivities to nitrogen and water addition vary among microbial groups within soil aggregates in a semiarid grassland. *Biol. Fertil. Soils* 53, 129–140. <https://doi.org/10.1007/s00374-016-1165-x>.
- Yan, F.L., Shi, Z.H., Li, Z.X., Cai, C.F., 2008. Estimating interrill soil erosion from aggregate stability of ultisols in subtropical china. *Soil Tillage Res.* 100, 34–41. <https://doi.org/10.1016/j.still.2008.04.006>.
- Zhang, Q., Zhou, W., Liang, G., Sun, J., Wang, X., He, P., 2015. Distribution of soil nutrients, extracellular enzyme activities and microbial communities across particle-size fractions in a long-term fertilizer experiment. *Appl. Soil Ecol.* 94, 59–71. <https://doi.org/10.1016/j.apsoil.2015.05.005>.
- Zhao, D., Xu, M.X., Liu, G.B., Yao, X., Tuo, D.F., Zhang, R.R., Xiao, T.Q., Peng, G.Y., 2017a. Quantification of soil aggregate microstructure on abandoned cropland during vegetative succession using synchrotron radiation-based micro-computed tomography. *Soil Tillage Res.* 165, 239–246. <https://doi.org/10.1016/j.still.2016.08.007>.
- Zhao, D., Xu, M., X Liu, G. B, Ma, L., Zhang, S., Xiao, T. Q. & Peng, G. Y., 2017b. Effect of vegetation type on microstructure of soil aggregates on the Loess Plateau, China. *Agric., Ecosyst. Environ.*, 242, 1–8. <http://doi.org/10.1016/j.agee.2017.03.014>.
- Zhao, G., Mu, X., Wen, Z., Wang, F., Gao, P., 2013. Soil erosion, conservation, and environment changes in the loess plateau of china. *Land Degrad. Dev.* 24, 499–510. <https://doi.org/10.1002/ldr.2246>.
- Zhong, Y.Q.W., Yan, W.M., Wang, R., Wang, W., Shangguan, Z.P., 2018. Decreased occurrence of carbon cycle functions in microbial communities along with long-term secondary succession. *Soil Biol. Biochem.* 123, 207–217. <https://doi.org/10.1016/j.soilbio.2018.05.017>.
- Zhu, G.Y., Deng, L., Zhang, X.B., Shangguan, Z.P., 2016. Effects of grazing exclusion on plant community and soil physicochemical properties in a desert steppe on the Loess Plateau, China. *Ecol. Eng.* 90, 372–381. <https://doi.org/10.1016/j.ecoleng.2016.02.001>.
- Zhu, G.Y., Shangguan, Z.P., Deng, L., 2017. Soil aggregate stability and aggregate-associated carbon and nitrogen in natural restoration grassland and Chinese red pine plantation on the Loess Plateau. *Catena* 149, 253–260. <https://doi.org/10.1016/j.catena.2016.10.004>.
- Zhu, G.Y., Deng, L., Shangguan, Z.P., 2018. Effects of soil aggregate stability on soil n following land use changes under erodible environment. *Agric. Ecosyst. Environ.* 262, 18–28. <https://doi.org/10.1016/j.agee.2018.04.012>.
- Zhang, W., Qiao, W., Gao, D., Dai, Y., Deng, J., Yang, G., Ren, G., 2018. Relationship between soil nutrient properties and biological activities along a restoration chronosequence of *Pinus tabulaeformis* plantation forests in the Ziwuling Mountains, China. *Catena* 161, 85–95. <https://doi.org/10.1016/j.catena.2017.10.021>.